Multi-objective optimization of building integrated photovoltaic solar shades

Seyedsoroush Sadatifar[a], Eric Johlin[a]

[a]*Western University, 1151 Richmond St, London, N6A 3K7, Ontario, Canada*

Abstract

Building-integrated photovoltaic (BIPV) systems allow solar panels to perform additional functions beyond energy generation for buildings, such as regulating interior lighting conditions and incoming radiative heat. However, optimizations of BIPV solar shades generally do not consider all of these factors, instead often focusing on power production alone. In this work, we explore a design framework for optimizing the configuration of BIPV shading devices to maximize a combination of power generation, interior daylighting quality, and radiative heating and cooling loads. This is applied to a simple room in five different locations and climates, as well as a case study of an office building. The low computational cost of this model allows for the full mapping of the influence of all design parameters on the value of the system, while demonstrating less than 7% error in predicting the performance of a benchmark experimental system. It is observed that the location and building geometry have significant influences on the relative values of heat, daylighting, and power production, with the overall combined value varying by up to 40% between the compared climates. The optimal design in many locations depend on user preferences as well, with many efficient solutions possible for varying trade-offs between the values of natural light vs. energy savings (a difference of up to 50%), as well as the system upfront cost vs. performance, further reinforcing the importance of tailored building-specific design for BIPV solar shades.

1. Introduction

Photovoltaics (PV) are one of the fastest-growing segments of the renewable energy industry (Debbarma et al., 2017). Building-integrated photovoltaic (BIPV) systems represent a way to expand the beneficial aspects of PV, allowing buildings partially meet their power needs by generating electricity (Biyik et al., 2017) and thereby reducing their environmental impact (Ravyts et al., 2020). BIPV utilizes photovoltaic materials to replace conventional building components such as window covers and shades, facades, and roofs, helping to reduce the cost of PV by using the solar cell structure for an additional purpose (Peng et al., 2011).

There are three main factors that window-mounted BIPV systems can directly influence: the quality of interior daylighting (Yoo, 2019; Ghosh et al., 2020), the radiative heat transfer through the windows, and the power generation by the PV system (Zhang et al., 2017; Alrashidi et al., 2019). These factors are all fully interconnected, as they all depend on how the incoming sunlight toward the window is managed by the BIPV system. The incoming light however is a function of the local climate and weather conditions, as these factors vary both the distribution of both direct and diffuse incoming light (in power, angle, and timing), as is the relative benefit of heat. An ideal BIPV system would thus need to maximize this inextricable trade-off between increasing produced power, reducing detrimental lighting conditions and warm-weather heat gain, while also increasing beneficial lighting conditions and cold-weather heat gain.

While the full optimization of a BIPV shade considering heat, power, and daylighting is thus needed, this previously has not been performed. Prior studies on optimization of BIPV shading devices have generally focused on tuning of either one (Yoo, 2019; Zhang et al., 2017; Sun et al., 2015, 2012; Asfour, 2018; Paydar, 2020) or two design parameters (Bahr, 2014; Taveres-Cachat et al., 2019, 2017; Nielsen et al., 2011), usually optimizing angle, as well as either the number or length of shades, but not both.

The majority of these investigations are additionally single-objective optimizations as well, focusing on maximizing the electricity production of the PV system alone. When the influences of building heating or cooling are considered, this is usually restricted to the influence of shades on the cooling load reduction, with potential detrimental effects on increasing the heating load during cold weather being neglected (Zhang et al., 2017). In systems that consider interior lighting performance, the analysis of daylighting has

been purely in terms of energy saving, and the user preference for natural light over artificial light has not been considered. Previous works have also generally not considered the influence of diffuse and direct light separately in terms of interior daylighting quality, and thus the negative influence of glare (from direct light) could not be fully captured (Bahr, 2014). Finally, most works consider a single location for their analysis, obscuring the dependence of the specific chosen environment on the analysis.

These limitations largely arise from the computational cost of the simulations needed to predict system performance. While BIPV systems generally have very simple geometries, often full 3D modelling software is utilized to calculate the system performance (Xie et al., 2018). This, combined with the large number of calculations that are needed to fully map a design space make such investigations impractical, particularly when comparing multiple locations and climates.

Herein, we work to address all of these current limitations, by combining a multi-objective optimization with multi-parameter design of a louvered BIPV shading system. This framework considers the impact of electricity generation from the crystalline silicon solar cells, heating load modifications (both beneficial and detrimental) from the change in direct and diffuse light transmitted through the window, as well as modifications to the interior lighting conditions in both direct and diffuse light intensities. This is performed by a simple but accurate model tailored to the specific geometry of this system. The individual performance factors are then combined into an overall value function of the system, and optimized through the design of the length, angle, and number of photovoltaic shades in a BIPV system for a specific location on earth, considering both local lighting conditions as well as weather.

The main results generated from this model are threefold: First, we demonstrate that historical average data can provide superior optimization results when compared to more commonly used high resolution single-year data. Second, we demonstrate how both location and design constraints can lead to vastly different trade-offs both between lighting quality and power optimization, as well as system complexity and value. And finally, we show how building parameters can significantly influence the final optimization, not only in specific optimal values, but even in the trade-offs between parameters. Overall, these results motivate the need for frameworks such as the one developed herein for building-specific optimizations of solar shade installations.

3
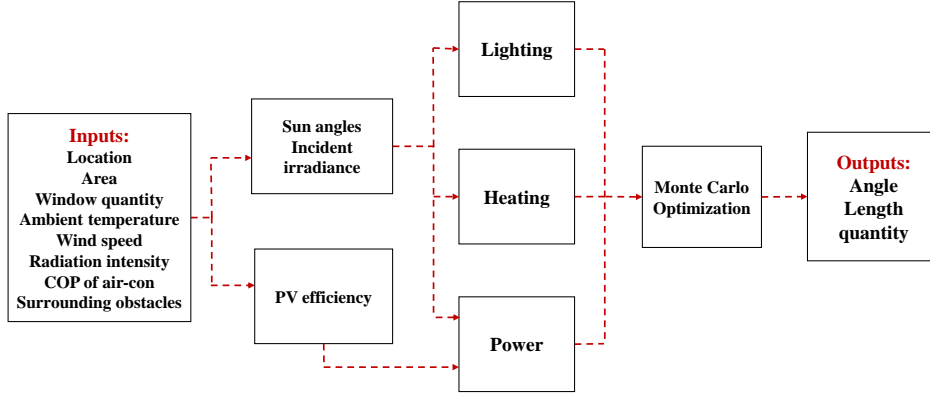
Figure 1: Schematic flowchart of the model framework, showing input data, optimized parameters, and final design specification outputs.

2. Methodology

Generally, the optimization framework developed herein works by combining a geometric model of the BIPV shade with both measured data on weather and insolation, as well as empirical relationships governing photovoltaic performance. This begins by the system taking in design constraints, weather and radiation data of a specific location, building properties and orientation, solar cell properties, and other optional environmental effects such as surrounding obstacles. The overall value of the design is maximized with a multi-objective optimization which takes into account three factors: the power generation of PV panels, the radiative heat transfer into the building, and the interior lighting quality. It is then able to provide optimum design parameters of the BIPV shading system consisting of the angle, length, and number of the shades on each window. Fig.1 displays an overall flowchart of the methodology of the framework studied in this work.

2.1. Geometric Modeling

In order for full optimization of the three design parameters and multiple objectives considered here to be feasible, the model must be computation-

ally inexpensive. For this reason, we consider a simple geometric model of the shade, combined with historically measured data for the insolation and environmental conditions of the location of interest, and empirical fits to experimental data for the PV performance. This allows the most significant factors influencing the performance of the solar shade to be considered, without the need for prohibitively expensive full daylighting or optoelectronic PV simulations to be performed.

The geometric model of the window and BIPV shades is summarized in Fig. 2, showing both direct and diffuse light contributions passing through the window in Fig. 2 (a) as well as on the photovoltaic shades in Fig. 2 (b). Full details of the calculations of the flux on each surface are given in the Supporting Information.
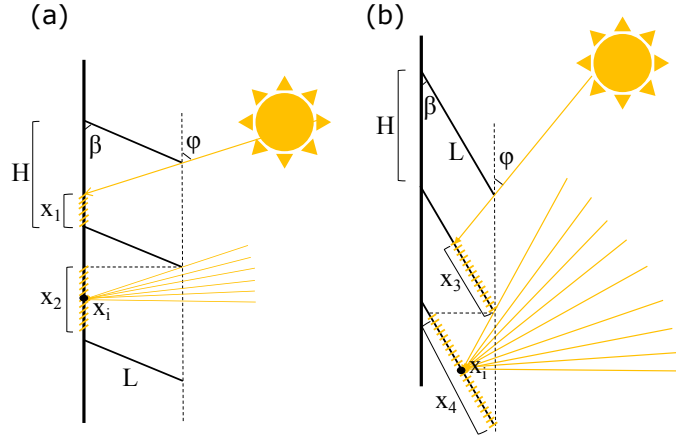
Figure 2: Areas exposed to direct and diffuse radiation (yellow hashed regions) for windows (represented by the vertical line), and shades (represented by the three slanted lines), in (a) and (b), respectively. Both are functions of the solar angle ϕ, shade angle β, distance between shades (H) and shade louver length (L).

2.2. Energy Modeling

The energy modeling in this framework consists of three separate components: electricity produced by the PV cells, heat transferred through the window, and daylighting inside the building.

The electrical output of the PV cells is determined both by the average light intensity on the panels, as well as the thermal environment. The influence of solar cell temperature, wind speed, and radiation intensity on the module efficiency are included using fits to empirical models (Schwingshackl

et al., 2013; Mattei et al., 2006; Reich et al., 2005). We here utilize mono-crystalline silicon as the PV material due to its current market dominance. These relationships are incorporated into the weather-dependant efficiency, η, modifying the base PV power conversion efficiency of 17.9%. Details of these parameters are given in the Supporting Information.

The amount of electricity production by panels, (E_{gen}), is determined by the product of the illuminated area (a_s, calculated from the appropriate lengths, $X_{3,4}$ as shown in Figure 2, and the width of the shades), the insolation (I_{POA}) and the cell efficiency (η) as

$$E_{gen} = n_s(a_s I_{POA} \eta) \tag{1}$$

This is then multiplied by the total number of shades (n_s) to get the total energy production.

The amount of thermal energy passing through the windows is determined similarly by the insolation, illuminated window area (a_w), and transmittance of the windows (T_w) as

$$H_{gen} = n_w(a_w I_{POA} T_w) \tag{2}$$

The transmission factor of the window is taken to be 79.3% (T. Chow and Lin, 2010). This heat transmission can be either desirable or undesirable depending on the local temperature, which is incorporated in the value functions, discussed below.

The light that comes through the windows consists of two parts: beam (direct) light and diffuse light. Generally, natural diffuse light is always considered desirable, while beam light causes glare, which can be undesirable if the intensity is too high. Sunshades are often designed to allow sufficient diffuse light into the room, while preventing excessive beam light to reduce glare. The intensity of beam (L_b) and diffuse light (L_d) are thus calculated separately, as

$$L_{b,d} = n_w \frac{I_{b,d} a_{b,d}}{0.0079 a_f}. \tag{3}$$

Here, a_b and a_d are window areas exposed to beam and diffuse light, respectively, and a_f is the total area of the floor space. The factor 0.0079 is the approximate conversion coefficient of lux to $\frac{w}{m^2}$ (1 lux = 0.0079 $\frac{w}{m^2}$) (Michael et al., 2020) and is explained below. Additional details on this modelling framework are provided in the Supporting Information.

2.3. Optimization

Four value functions are defined for optimization, accounting for power generation, incoming heat, and lighting quality. Each value function can be used as a criterion for optimization alone, or in combinations together. The value functions correspond to the total value of that energy source over the course of the year.

First, the power value function is defined as the amount of electricity produced by the PV cells during a year, calculated as the sum over the hourly electricity generation for the year,

$$V_P = \sum_{h=1}^{8760} E_{gen}.$$ (4)

While generating electricity is always desirable, incoming heat through windows is only preferable when outdoor temperature is below the desired room temperature. On warm days, any incoming heat is treated as needing to be removed by the building's cooling system, and thus negating the benefits of some power generation. These effects are incorporated with a coefficient (C_P) corresponding to if heat is considered to have positive or negative value. The value of (C_P) is determined by the coefficient of performance of the building HVAC system, with a negative sign when the external temperature is over 20°C, positive sign when less than 18°C, and set to zero at temperatures between these values. Accordingly, the heat value function is calculated as the summation of the value-weighted heat passing through windows every hourly time step for the year,

$$V_H = \sum_{h=1}^{8760} C_P H_{gen}.$$ (5)

Similarly, the lighting value also can be positive or negative, and a lighting coefficient is used to weight the light value function. Diffuse light is considered to always be beneficial, while direct is undesirable due to glare production, particularly if the intensity is too high. According to the LEED® standard, the favorable overall range of light in an office environment is between 300 *lux* and 3000 *lux*. Accordingly, the diffuse light coefficient (c_d) is always positive and increases linearly to a value of 1 for diffuse light at 300 *lux* in the room. The direct light coefficient (c_b) is negative and decreases linearly with the direct light intensity, saturating at a value of -2 if the direct

light is more than 3000 *lux* in the space, corresponding to an unacceptable level of glare. These values are chosen so that the optimization will still penalize large amounts of total (direct + diffuse) light passing through the window. Finally, an additional coefficient, (γ), is also defined to account for user preference of natural light vs. artificial light. The light value function (V_L) is thus defined to be

$$V_L = \gamma \sum_{h=1}^{8760} (c_b L_b + c_d L_d) P_L a_f \tag{6}$$

where P_L is the average amount of power needed to light a space with no natural light, and for an office room is around $2.5 \frac{w}{m^2}$. With $\gamma = 1$, the V_L is simply the power savings from artificial lighting being offset by natural light, $\gamma < 1$ would indicate a (unlikely) preference for artificial light, and $\gamma > 1$, a preference for natural light. Here γ is taken to be 3, as this is found to give reasonable trade-offs with the other value functions, as discussed below.

While any of the three above value functions could be used alone, it is most useful to combine power, heat and light together in one overall value function (V_O) to optimize the interplay between these components. The overall value function is converted into units of dollars based on the price of the electricity, P_E, to allow easier comparison to the other costs, such as the price of the equipment, and is defined as

$$V_O = P_E(V_P + V_H + V_L) \tag{7}$$

where P_E is assumed $0.13 \frac{\$}{kWh}$ and the unit of V_O is in $\frac{\$}{year}$.

A stochastic Monte Carlo optimization method (Glynn, 1986) is used to find the best combination of angle, length, and quantity of shades for each window. This method generates random sets of values for design parameters within fixed bounds in every iteration until it converges to optimum results, and is chosen for its simplicity and low computational cost. Furthermore, it allows more complete comparison of the trade-offs between different parameters than a more complex (e.g. gradient-based) optimization strategy. For more details, see Supporting Information section S3.

For each stochastically generated parameter combination, the optimization runs by stepping through each hour of the year, utilizing the empirical weather and insolation information to compute the hourly contribution to each value function. The sum of the hourly contributions yields the overall performance of the specific combination of angle, length, and number of
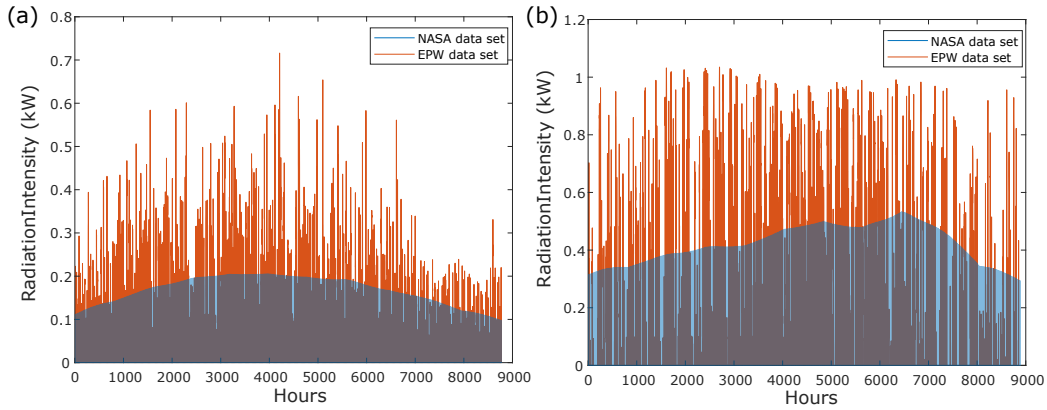
Figure 3: Comparison of insolation data for two data sets – historical monthly averages (NASA data set, blue) and single-year hourly data (EPW data, red) of **(a)** diffuse radiation **(b)** direct radiation for London, Canada over a year.

shades. Here, we limit the shade length to 50 cm, and the total area of shades equal to the window area. Angles can vary from 0° (fully closed) to 90° (parallel to the ground), and the number of shades is limited only by the above limits on total length and area.

2.4. Input Data

In order to calculate the incoming solar radiation, two data sets were considered. The first data set is monthly averages taken from the NASA POWER Project (NASA, 2020), referred to here as the "NASA" data set. These data are averages of 30 years (Jan 1984 - Dec 2013) and since the available data are only monthly averages, in order to estimate hourly radiation intensity, the monthly averages are first interpolated to daily values. To account for variations with each day, an expected hourly radiation profile is calculated based on the air mass at the corresponding solar angle (Meinel and Meinel, 1976), and then normalized so that it integrates to the historical daily value.

The second data set is provided by EnergyPlus, generally referred to as "EPW" data. The EPW data are much higher resolution hourly measurements, but only taken from one arbitrary year, which varies with location. Fig. 3 compares the diffuse and direct radiation intensity in NASA and EPW data sets for London, Canada, with the former data depicted as the shaded blue region, and the latter as the orange lines. It is clear that the EPW data has significantly larger peaks and troughs, since these data are collected from

a single year leading to increased variability, while the NASA data is more smooth, due to the 30 year averaging.

Initially, neither data set is convincingly optimal over the other, as one could imagine that either the high variability of a single year data set at hourly intervals would provide the most accurate representation of the actual isolation conditions of a location (important for the non-linear response of PV efficiency included here), but also could suffer from potentially being non-representative of a normal (long-term average) condition. For this reason, we compare our optimization on both data sets to determine the influence of using historical *vs.* single-year data, as discussed below.

2.5. Model Validation

In order to validate the accuracy of the model developed here, predictions from the present work are compared to both a range of simulation data from Energy3D software (Xie et al., 2018), as well as experimental measurements of a large scale BIPV installation. Energy3D allows full three-dimensional modeling, rendering, and simulation of photovoltaic installations, but at a much higher computational cost (0.2 seconds/simulated day, *vs.* 0.11 milliseconds/simulated day for the present work, or almost 2,000× slower).

First, the power production of a single $1.2m \times 0.6m$ monocrystalline silicon panel with a power conversion efficiency of 18% is compared in five different angles in three different locations (Los Angeles, Berlin and Singapore). Simulations are run testing both single shades on the south wall of a building in Figure 4 (a), as well as shades with self-shading effects in Figure 4 (b). It is observed that the trends both for changing the angle within each location, as well the relative performance between cities agree qualitatively very well. The two simulations utilize different sources of weather (radiation, temperature, and wind speed), so exact agreement would not be expected. Overall, we observe mean differences of 10% for un-shaded panels, and 18% for self-shading. It is important to note that much of this difference is due to the model developed here predicting uniformly lower values than Energy3D. This is likely due to the present work including the non-linear influence of mean insolation on PV efficiency, more detailed weather data (separating specific direct and diffuse light contribution), as well as a more detailed temperature model for PV efficiency (utilizing local wind speeds as well as insolation and ambient temperatures).

The higher accuracy of the present model is demonstrated through comparison with experimental data from (Lee et al., 2017) for a case study of
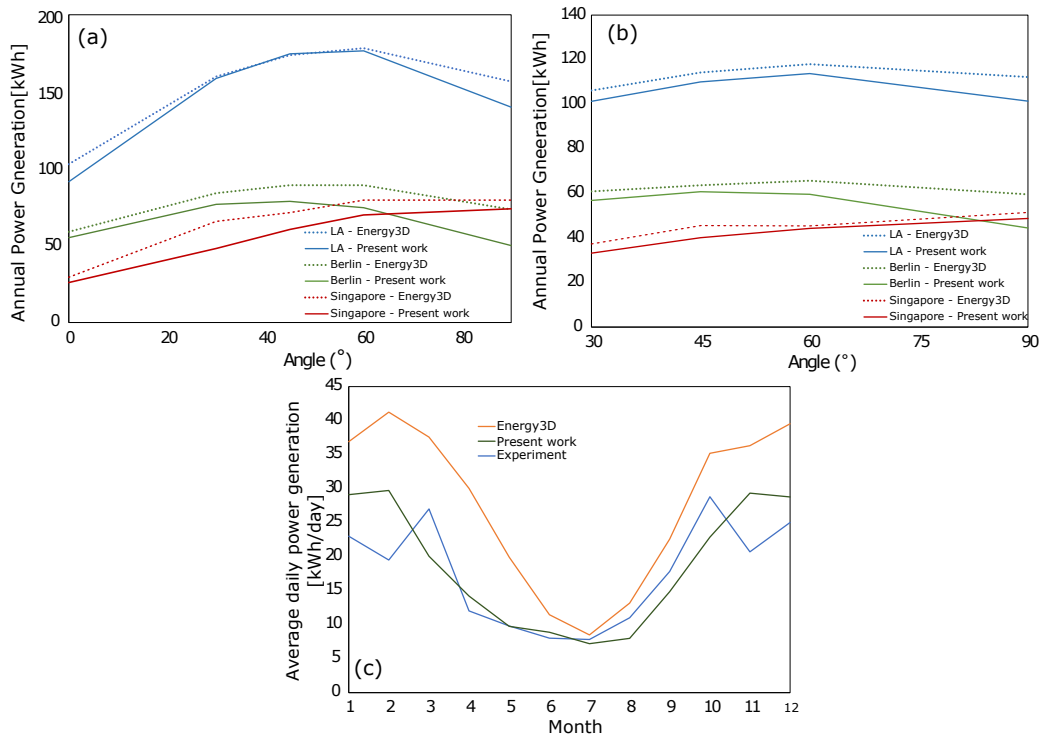
Figure 4: Total power generation comparison between the present work and existing PV simulation software. Comparisons between a single shade at a range of angles between the shade and the south wall of a building, when **(a)** un-shaded, and **(b)** self-shaded by an equal sized shade 0.5 m above. **(c)** Comparison of simulation results of the present work to existing Energy3D software and experimental data (Lee et al., 2017).

a BIPV installation in South Korea in Figure 4 (c). The results show that while the general shape of the two models and experimental data all agree fairly well, the present work fits significantly better with the experiment, with the higher complexity Energy3D model significantly over-predicting the power output, particularly in the first half of the year. This indicates that the lower energy generation the present work calculates in (a) and (b) may indeed be more accurate as well.

Finally, we note that even without any specific experimental data input into the model, using only solar panel specifications and general location information, our work is still able to predict the total observed annual power generation with less than 7% error, especially significant when compared to the 60% error produced by existing software.

3. Results and Discussion

We begin our investigation of this optimization process by comparing the influence of the two data sets mentioned above, the NASA and EPW data sets. Then, we discuss the results for the simple case study in five different locations, and finally a realistic office case study.

3.1. Simple Room

We first explore the optimization for a simple example room with a square 55 m^2 footprint, no obstructing surroundings, and with two south-facing and two east-facing windows of area 1.51 m^2, schematically depicted in Figure 6 (a), in five different locations: London, Canada; Tehran, Iran; Los Angeles, USA; Berlin, Germany; and Singapore. These locations were chosen as representatives of different geographical locations and climates on earth. The overall variations in value of the systems are as high as 40% between the varied climates.

The optimization is run for the example room in these five different locations to calculate the optimum design configurations for both NASA data (30 year average) and EPW data (1 year of high-resolution data). Next, model is re-run to calculate the overall value function (V_O) of the system with both data sets for each of the two design configurations. As seen in Figure 5 (a), both configurations (the two columns for each location) show quite similar performance, as does each data set (red and green bars within one column), despite their significant differences on an hourly basis.

While each configuration by definition will perform better on its own data set, it is useful to investigate if one configuration performs better on the alternate data set than the other – this can indicate if it is more important to incorporate long term averages (NASA data) or to include the more significant fluctuations within a single year (EPW data) in the optimization. We observe that the long-term average (NASA data set based) configuration shows slightly better performance on the EPW data set (99%), when compared to the one-year (EPW data set based) configuration when analyzed using the NASA data set (97%). This indicates that generally basing the optimization on a long term average yields a design that will perform better both on a specific year, as well as in the long term average, than basing the optimization on the more significant fluctuations within a sample year. In light of this, all subsequent optimizations are based on the NASA data.
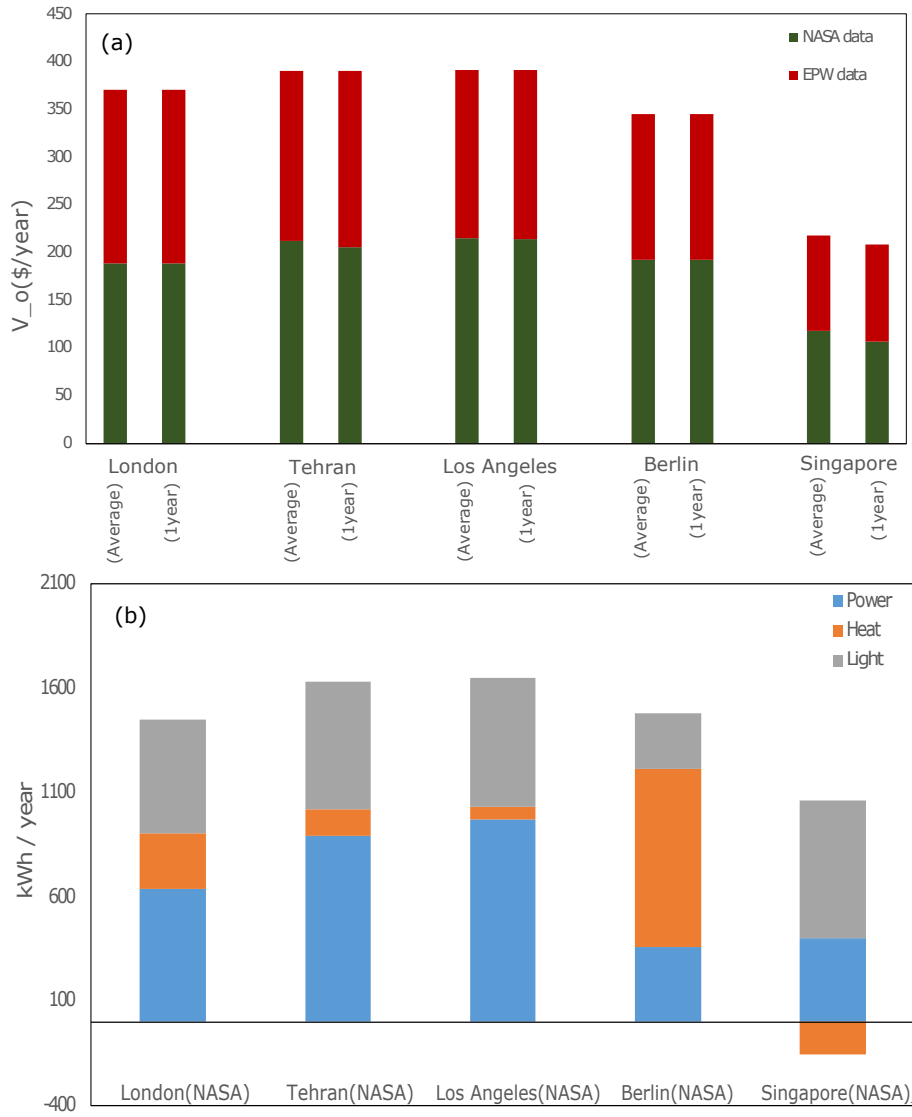
Figure 5: Comparison of NASA and EPW data sets for five different locations. **(a)** overall value function of simple case for NASA and EPW data set in both average and single year configuration **(b)** energy breakdown of simple case with NASA data set.

We next examine the contribution of the specific value functions to the V_O of the Average configuration in Figure 5 (b). It can be seen that in warmer locations (Tehran and Los Angeles) the power production has higher value, but in colder locations (Berlin) heat can significantly exceed the value

of power production. In tropical locations (Singapore), where sun is higher in the sky, blocking direct light to prevent heating and providing comfortable daylighting conditions offers the most value. This is likely due to more substantial self-shading of the solar louvers preventing significant power production. This also highlights that while locations can have very similar values of V_O (e.g. London and Berlin), the components of the value functions can be significantly different.

In order to better understand the trade-offs generating these varying optima in V_O, we explore the optimization of the London, Ontario (Canada) location in detail. Figures 6 displays the variation of the overall value function in different sets of design parameters for 200,000 iterations, with each iteration plotted as a single point in each figure, and corresponding to one specific combination of design parameters (length, number, and angle of shades). Each parameter is isolated in a separate sub-figure (b-d) to investigate the influence of that parameter, while the variation of the other parameters is visible through the vertical spread of the points. The optimum configuration is thus the point at the highest vertical position in each sub-plot, from which the ideal value for each parameter can be found.

As seen in Figure 6 (b), when the shades are at the angle of $\beta = 65°$ to the window, the system will be at its maximum overall value. Although panels generate more electricity at smaller angles, this would cause the room receive less diffuse light and heat, indicating that the heat and light value functions are pushing the optimum condition to higher angles.

Figure 6 (c) and (d) also illustrate that highest overall value function is achieved by using 3 shades with a length of 50 cm. As the number of the shades increases, the overall value function decreases. This is likely due to an increased number of shades allowing less light and heat into the room, as well as causing significant self-shading of the panels – upper panels block light to the lower panels, especially when the sun is high. Therefore, only the leading edge of the solar cells will receive both direct and diffuse light. This effect is further compounded by the cell efficiency falling with decreasing average illumination as well, further reducing the power production.

While the optimization shown here was done by requiring the south and east side windows to have the same configuration, the different directions can also be independently optimized. However, if two directions are allowed to have different configurations, we see that there is only a 2.52% difference in V_O. We thus keep the configuration the same for both directions for the simplicity of the design.
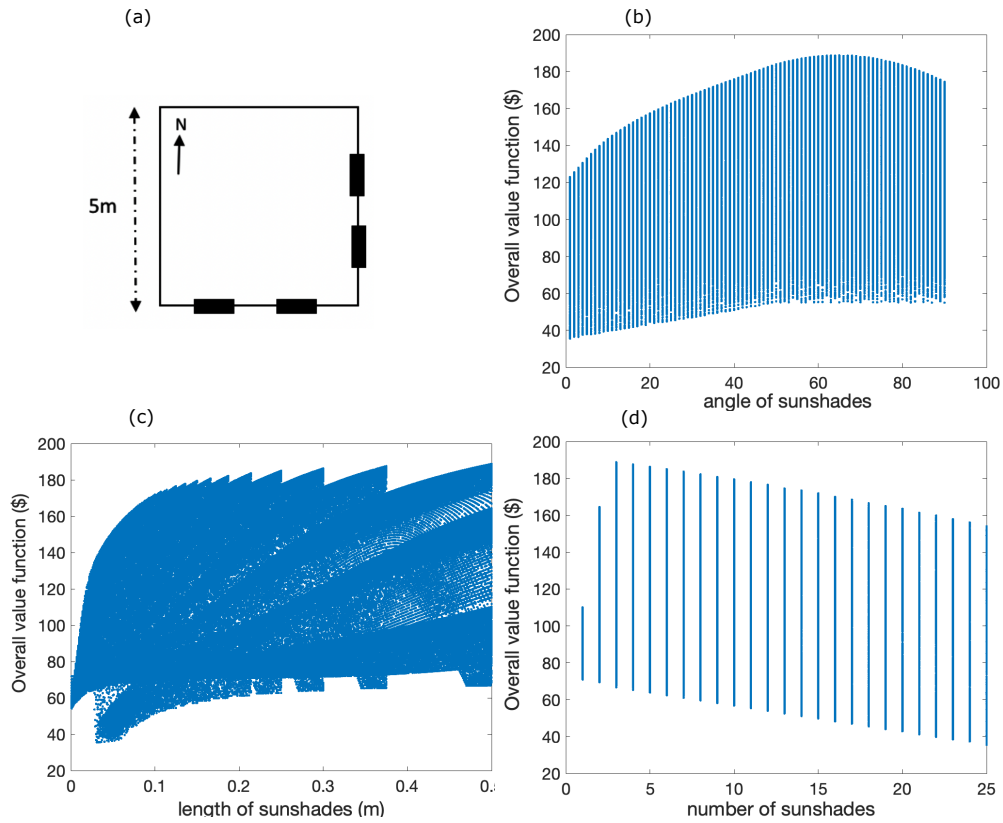
Figure 6: Optimization of the simple room solar shade for the example location of London, Ontario (Canada). **(a)** Schematic of the simple room, with windows on the south and east walls, denoted by thick black lines. Optimization profiles, with each point representing a single configuration, showing the response of the overall value function to changes in **(b)** angle **(c)** shade louver length and **(d)** number of the shades. The overall optimal configuration corresponds to the vertical maximum of each plot.

Table 1: The optimal design parameters for the simple room in all five studied locations.

Location	London, Canada	Tehran	Los Angeles	Berlin	Singapore
Latitude	42.98°N	35.68°N	34.05°N	52.52°N	1.35°N
Angle	65°	57°	54°	90°	42°
Number	3	3	3	3	6
Length	50 cm	50 cm	50 cm	50 cm	25 cm

15
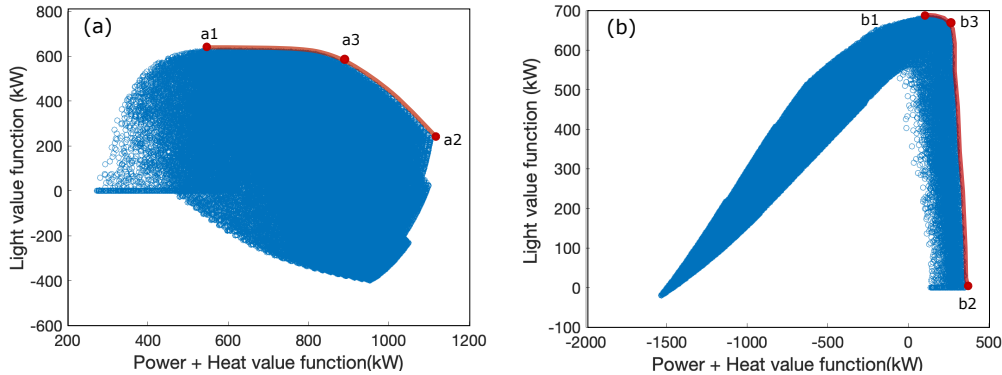
Figure 7: Comparison of trade off between the light and heat+power value functions for the simple case study in **(a)** London (Canada), and **(b)** Singapore. Red lines indicate the efficient solutions, with single-objective optima points indicated at each end (a1, a2, b1 and b2). Points a3 and b3 are optima points for the presently used value of $\gamma = 3$.

The optimal design parameters are listed in Table 1 for all five cities. A few trends between these values are apparent – in non-tropical environments (all but Singapore), the optimal design shows a common 3 shades of 50 cm length. This corresponds to the maximum amount of shade material, given that shades are at their maximum length. This allows the minimization of self shading by maximizing the distance between shades, while still utilizing the maximum area of PV material allowed. In warm climates (Tehran, and Los Angeles), a lower angle allows for more significant blocking of radiant heat, while colder climates increase the angle to improve heat gains in the winter (lower solar angles) while still blocking more light in the summer (higher solar angles). Singapore shows that even more significant blocking of incoming radiation to the windows is optimal, doubling the number of shades at half the length, and lowering their angle. Even with this, the heat function is still negative, as seen in Figure 5.

While power generation and heat flux can be clearly quantified, lighting quality cannot, as it depends on the user preference for natural light. This leads to a potential trade-off, and that different user preferences can lead to different optimal configurations. Figure 7 displays different configurations with their associated energy savings (the sum of beneficial heat and power generation of the system) and light value functions for the cities of London, Canada in (a) and Singapore in (b), chosen for their significantly different climates. In this figure, each point represents the design configuration of

16

shades, and each point on the red line can be considered an efficient solution that can be optimal for different preferences of the relative value of daylighting quality.

As seen in Figure 7 (a), if lighting quality is considered significantly more valuable than energy (power + heat), point (a1) is the optimal configuration; conversely, if there is no consideration for lighting quality, the energy savings are maximized at point (a2). The exterior region between point (a1) and (a2) (shown with the red line) represents efficient solutions for any decision where there is preference both for improved lighting quality and energy savings, at varying relative values. It can be seen that by changing the relative value of lighting, the optimal energy production is varied by a factor of more than 50%. For the relative value of natural lighting over artificial lighting considered here ($\gamma = 3$), (a3) is the optimum condition.

Figure 7 (b) shows a similar trade-off for Singapore. However in this case, the line of efficient solutions is far more narrow, showing that in order to slightly improve energy savings, there must be a significant reduction in lighting quality. Furthermore, the optima (b1) indicates that if lighting quality is of the highest importance, it may not be feasible to use photovoltaic shades, due to the low energy savings, and passive shades may be more cost effective. Finally, it should be noted that both V_L and $V_P + V_H$ can become negative, as glare and incoming heat on warm days respectively can both lead to negative value of the system.

3.2. Economic considerations

So far, we determined the optimum design configuration of BIPV shades, however in real installations, the recurring yearly value of the system must be weighed against the upfront cost. The relationships depicted in Figure 6 can be used to demonstrate trade-offs in performance when certain design constraints are implemented or modified. For example, if it was known that system cost would be reduced substantially by limiting the sunshade length to 25 cm (through reduced amount of support structures, etc.), Figure 6 (c) shows that reducing the louver length from the optimal 50 cm to 25 cm could still maintain 98% of the overall value, through adjustment of other design parameters. Similarly, if one was interested in comparing to a system with a single shade, it can be seen that the overall system value would be only 58% of the optimal configuration, while moving to two shades increases this to 87%. It is important to note that while the overall value function may

17

stay at a similar level between design modifications, the balance between the three specific value functions may change significantly.

One of the most significant contributions to the cost of any BIPV system is the photovoltaic cells utilized, which can account for more than 70% of the total system cost (Yang and Zou, 2016). In Figure 8 we explore specifically this trade-off between the overall value function (V_O) of the system and the amount of PV material utilized. As we would expect from the above discussion, the value monotonically increases with increasing PV area, however it is also now clear that the marginal benefit of increasing the amount of photovoltaic area on the shade system changes significantly. This is observable as the slope of upper surface of the distribution of designs. One can see the slope along the upper surface in London (a) first increases and then decreases as the amount of PV area increases, but Singapore (b) shows two more obvious regions. It can also be seen that in Singapore in particular, the value largely plateaus around 2.5 m^2, indicating that even though the V_O keeps going up after this, the reduced slope indicates that a smaller system will still produce most of the value of a larger (more expensive) one. Specifically, we see that increasing the area for this system by a factor of 2.5$\times$ only increases the value of the system by less than 25%.

Furthermore, the value of the window without any shades is also denoted through the red circle on the zero PV area axis. This can either be pos-
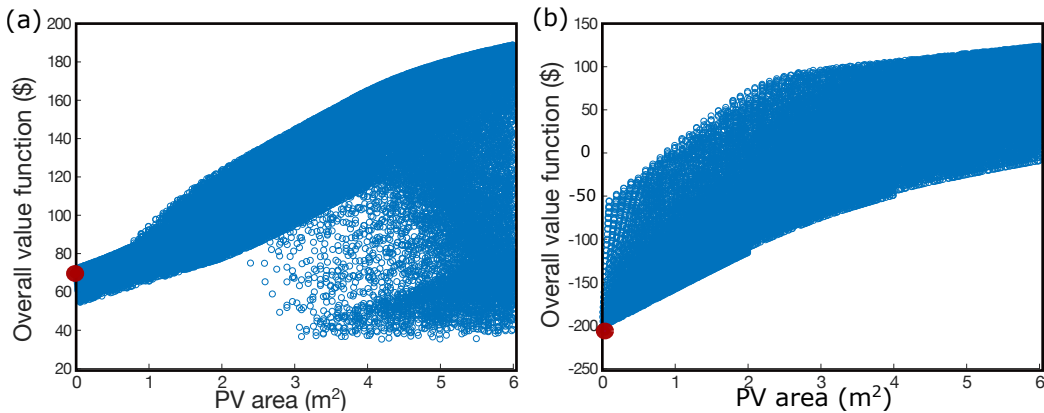
Figure 8: Overall value of the system shown as a function of the total area of PV shades used, for the cities of **(a)** London and **(b)** Singapore, with each blue point representing a different design solution. The value of windows without any shades is indicated by the larger red circle.

18

itive (as in the case of colder climates where having unobstructed window will allow significant heat gains) or negative (as seen quite significantly in Singapore). This means that the true value of going from a bare window to an optimized shade is actually the difference between the blue point and red circle, suggesting that while the absolute overall value in Singapore appears low, when taken relative to the significant negative value of having no window shades, the value is actually much higher (more than twice) that originally predicted, and even higher than other locations. Plots for the remaining cities are available in Supporting Information Figure S1.

While plots such as those in Figure 8 can help us understand the general trends in costs *vs.* value, the actual decision of which point is economically optimal will depend on the current price of PV cells and modules, installation and frame material costs, as well as the discount rate of the owner (how much more one values upfront costs relative to future savings). This further motivates the need for optimization methods such that presented here to be utilized individually for any specific building installation being considered.

3.3. Detailed Case Study

This model is finally implemented for conditions of a sample office building in London, Canada, allowing a realistic case study to be demonstrated. The office is located on the second floor of a building with an area of 380 m^2. The office has 10 windows, 7 south-facing and 3 east-facing. The area of each window is 3.6×2.1 m^2. A schematic of the office is shown in Figure 9 (a). To ensure a view for the office workers, 50 cm at the bottom of each window is fixed to be open, and not covered with any shades. The working time at the office is 8 am to 5 pm, and so the negative effect of direct light or positive effect of diffuse light as well as the effect of heating (either positive or negative) are only considered in this period of time, as it is assumed that the area is unoccupied outside of these hours. The coefficient of performance of the heating and air conditioning systems of the office are both taken to be 2 due to the use of heat pumps for climate control in the building.

The ideal parameters for this case study (those which maximize the overall value function) are to utilize two shades on each window, a shade length of 50 cm, and an angle of $\beta = 90°$ to the window. Figure 9 (b) displays the energy breakdown of the BIPV shading system of the office. Interestingly, this varies significantly from the simple room optimization shown above, as while the length of the shades is still at the maximum value, the number of shades is not. This is seen in the relative scale of the value functions as well, most

19
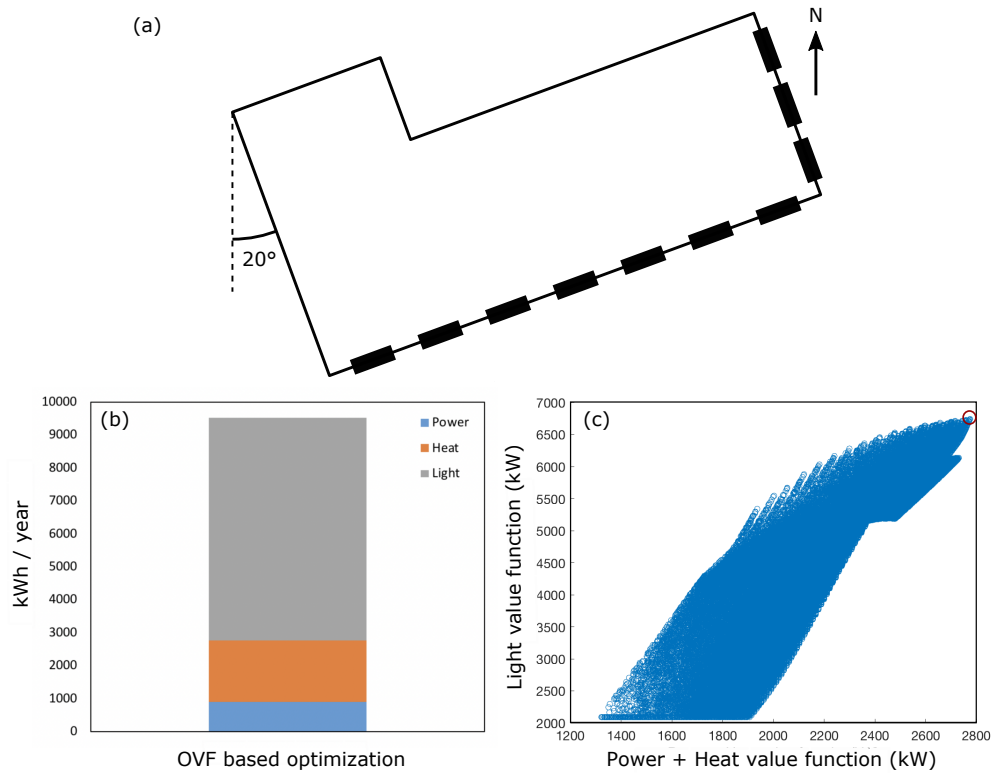
Figure 9: Case study optimization. **(a)** Schematic of the office, with windows shown as thick black lines. **(b)** Energy break-down for the optimal configuration. **(c)** Trade-off plot showing the interaction between light and power+heat value functions, with the overall dominant solution indicated by the red circle.

dramatically in the impact of the light value function. This demonstrates the strong sensitivity of the optimization to the specific configuration of the building being considered, and motivates the case for building-specific design of PV solar shades.

As seen in Figure 9 (c), the configuration generating maximum energy (electricity and beneficial heat) also has the highest light value function, indicating a single dominant solution, and that the optimized configuration is therefore independent of the choice of γ. This also differs significantly from the simple room example, indicating that not only the optimal condition, but the interaction between the different objective functions varies strongly with building-specific parameters.

Overall, this optimized system would use 3.8 kW of photovoltaic cells, and

shows a generation of \$1,237 in value per year. Based on the cost of electricity and the historical energy usage of the specific office, this corresponds to 15% of the total yearly energy costs for the office.

4. Conclusions

Herein we have developed an efficient computational model to optimize the configuration of photovoltaic sunshades while maximizing the combined value of incoming radiative heat, PV power production, and interior lighting quality. The consideration of both beneficial and detrimental heat gain, as well as the separation of direct and diffuse light are essential to the accurate calculation of system value, as is the recognition of different values between natural and artificial light.

A general trend is observed that in non-tropical climates the value of BIPV systems increases as fewer, longer shades are utilized, and with the optimal angle determined by the the particular location and building specifications. While this trend can help motivate the overall design of BIPV shades, we show that the trade-offs between cost and complexity, as well as lighting quality and energy savings motivate a need for location- and building-specific optimization of the system.

The ability of this model to fully map the design space also provides benefits to optimization, allowing direct exploration of the impact of varying design constraints on the overall value of a system. This can facilitate specific building-tailored design of BIPV solar shades by allowing systems of differing design constraints to be compared, and considered along with the corresponding changes in system cost, complexity, and aesthetics. This proves particularly useful as in some locations (e.g. Singapore, studied here) significant reductions in parameters such as the total PV area still maintain much of the system value. Finally, comparison to the proper initial condition (e.g. un-shaded windows for retrofit applications, or a lack of windows for new buildings) can additionally offer significant differences (by a factor of two or more) in some locations, again reinforcing the need for location-tailored design.

5. Data Availability

Data used for the optimizations herein can be found at the NASA POWER project, available at `https://power.larc.nasa.gov`.

6. Acknowledgements

References

Alrashidi, H., Ghosh, A., Issa, W., Mallick, N.S.T.K., Sundaram, S., 2019. Evaluation of solar factor using spectral analysis for cdte photovoltaic glazing. Materials Letters 237, 332–335.

Asfour, O.S., 2018. Solar and shading potential of different configurations of building integrated photovoltaics used as shading devices considering hot climatic conditions. Sustainability 10, 4373.

Bahr, W., 2014. A comprehensive assessment methodology of the building integrated photovoltaic blind system. Energy and Buildings 82, 703–708.

Biyik, E., Araz, M., Hepbasli, A., Shahrestani, M., Yao, R., Shao, L., Essah, E., Oliveira, A.C., del Caño, T., Rico, E., Lechón, J.L., Andrade, L., Mendes, A., Atlı, Y.B., 2017. A key review of building integrated photovoltaic (BIPV) systems. Engineering Science and Technology, an International Journal 20, 833–858.

Debbarma, M., Sudhakar, K., Baredar, P., 2017. Comparison of BIPV and BIPVt: A review. Resource-Efficient Technologies 3, 263–271.

EnergyPlus, . Weather data by location — EnergyPlus. URL: https://www.energyplus.net/weather. (accessed: 03.01.2021).

Ghosh, A., Bhandari, S., Sundaram, S., Mallick, T.K., 2020. Carbon counter electrode mesoscopic ambient processed and characterised perovskite for adaptive bipv fenestration. Renewable Energy 145, 2151–2158.

Glynn, P.W., 1986. Stochastic approximation for monte carlo optimization, in: Proceedings of the 18th conference on Winter simulation, pp. 356–365.

Lee, H.M., Yoon, J.H., Kim, S.C., Shin, U.C., 2017. Operational power performance of south-facing vertical bipv window system applied in office building. Solar Energy 145, 66–77.

Mattei, M., Notton, G., Cristofari, C., Muselli, M., Poggi, P., 2006. Calculation of the polycrystalline pv module temperature using a simple method of energy balance. Renewable Energy 31, 553–567.

Meinel, A., Meinel, M., 1976. Applied Solar Energy: An Introduction. Addison-Wesley Publishing Company.

Michael, P.R., Johnston, D.E., Moreno, W., 2020. A conversion guide: solar irradiance and lux illuminance. Journal of Measurements in Engineering 8, 153–166.

NASA, 2020. Nasa prediction of worldwide energy resources. URL: `https://power.larc.nasa.gov`. (accessed: 01.11.2020).

Nielsen, M.V., Svendsen, S., Jensen, L.B., 2011. Quantifying the potential of automated dynamic solar shading in office buildings through integrated simulations of energy and daylight. Solar Energy 85, 757–768.

Paydar, M.A., 2020. Optimum design of building integrated pv module as a movable shading device. Sustainable Cities and Society 62, 102368.

Peng, C., Huang, Y., Wu, Z., 2011. Building-integrated photovoltaics (BIPV) in architectural design in china. Energy and Buildings 43, 3592–3598.

Ravyts, S., Vecchia, M.D., Van den Broeck, G., Yordanov, G.H., Gonçalves, J.E., Moschner, J.D., Saelens, D., Driesen, J., 2020. Embedded BIPV module-level dc/dc converters: Classification of optimal ratings. Renewable Energy 146, 880–889.

Reich, N., Van Sark, W., Alsema, E., Kan, S., Silvester, S., Van der Heide, A., Lof, R., Schropp, R., 2005. Weak light performance and spectral response of different solar cell types, in: Proc. of the 20th EU PVSEC, pp. 2120–2123.

Schwingshackl, C., Petitta, M., Wagner, J.E., Belluardo, G., Moser, D., Castelli, M., Zebisch, M., Tetzlaff, A., 2013. Wind effect on pv module temperature: Analysis of different techniques for an accurate estimation. Energy Procedia 40, 77–86.

Sun, L., Hu, W., Yuan, Y., Cao, X., Lei, B., 2015. Dynamic performance of the shading-type building-integrated photovoltaic claddings. Procedia Engineering 121, 930–937.

Sun, L., Lu, L., Yang, H., 2012. Optimum design of shading-type building-integrated photovoltaic claddings with different surface azimuth angles. Applied Energy 90, 233–240.

T. Chow, C.L., Lin, Z., 2010. Innovative solar windows for cooling-demand climate. Solar Energy Materials and Solar Cells 94, 212–220.

Taveres-Cachat, E., Bøe, K., Lobaccaro, G., Goia, F., Grynning, S., 2017. Balancing competing parameters in search of optimal configurations for a fix louvre blade system with integrated pv. Energy Procedia 122, 607–612.

Taveres-Cachat, E., Lobaccaro, G., Goia, F., Chaudhary, G., 2019. A methodology to improve the performance of pv integrated shading devices using multi-objective optimization. Applied Energy 247, 731–744.

Xie, C., Schimpf, C., Chao, J., Nourian, S., Massicotte, J., 2018. Learning and teaching engineering design through modeling and simulation on a cad platform. Computer Applications in Engineering Education 26, 824–840.

Yang, R.J., Zou, P.X., 2016. Building integrated photovoltaics (bipv): Costs, benefits, risks, barriers and improvement strategy. International Journal of Construction Management 16, 39–53.

Yoo, S.H., 2019. Optimization of a BIPV system to mitigate greenhouse gas and indoor environment. Solar Energy 188, 875–882.

Zhang, W., Lu, L., Peng, J., 2017. Evaluation of potential benefits of solar photovoltaic shadings in Hong Kong. Energy 137, 1152–1158.